In reality the neighbours move and roughly these movements can be classified as 'in-phase' and 'out-of-phase'. For 'in-phase' movement the potential function is effectively softened, the mode frequencies are lowered and the amplitudes increased. This is not compensated fully by the 'out-of-phase' motions which correspond to raised frequencies and smaller amplitudes.

In the structures of benzene and sulphur the arrangement of neighbours is much more isotropic than in pyrene and phenanthrene. Comparison of the individual diagonal elements of **T** and **L** in the cases of benzene and sulphur shows no enormous discrepancy over and above a softening factor. However as the structure becomes increasingly anisotropic so the softening factor increases and detailed discrepancies appear.

The most striking discrepancy is in the value of T_{22} for pyrene. In this crystal pairs of molecules related by the centre of inversion lie on parallel planes distant 3·5 Å from each other, and they are almost perpendicular to the *b* axis. The close approach of so many atoms along this direction causes the potential to be very hard and the Einstein model gives a very small value, $T_{22}=0{\cdot}0098$ Å^2. The lattice-dynamical calculation yields a value of 0·0486 Å^2, which is in good agreement with the experimental value of 0·0369 Å^2. These experimental values come from the constrained refinement of neutron diffraction data (see Pawley, 1972*b*), and show a satisfactory overall agreement with the Born–von Kàrmàn calculation.

Thus it is possible to make qualitative arguments and conclusions using the diagonal elements of **T** and **L**. However no such argument can be used for the off-diagonal elements, including the elements of **S**. These are determined by the finer aspects of the molecular packing, and thus our understanding of intermolecular forces cannot be furthered by simple Einstein-model calculations. In many ways therefore our result is disappointing, but at least we learn to avoid making an assumption which is superficially plausible but which has no physical justification.

References

COCHRAN, W. & PAWLEY, G. S. (1964). *Proc. Roy. Soc.* A**280**, 1–22.

PAWLEY, G. S. (1967). *Phys. Stat. Sol.* **20**, 347–360.

PAWLEY, G. S. (1968). *Acta Cryst.* B**24**, 485–486.

PAWLEY, G. S. (1972*a*). *Phys. Stat. Sol.* **49**, 475–488.

PAWLEY, G. S. (1972*b*). *Advances in Structure Research by Diffraction Methods.* **4**, 1–64. Edited by W. HOPPE & R. MASON. Oxford: Pergamon Press.

SCHOMAKER, V. & TRUEBLOOD, K. N. (1968). *Acta Cryst.* B**24**, 63–76.

VENKATARAMAN, G. & SAHNI, V. C. (1970). *Rev. Mod. Phys.* **42**, 409–470.

Acta Cryst. (1973). A**29**, 663

Multiple Scattering and Dynamical Effects in Diffuse Electron Scattering

BY R. HØIER

Institutt for røntgenteknikk, Universitetet i Trondheim-NTH, N-7034 Trondheim-NTH, Norway

(*Received* 17 *April* 1973; *accepted* 30 *May* 1973)

A many-beam dynamical theory for Bragg scattering effects in diffuse electron scattering is developed which takes multiple diffuse scattering into account. For non-absorbing crystals the theory is shown to include previous theories for Kikuchi lines and bands; with absorption, a weaker dependence on the anomalous absorption parameters than in previous theories is found. The variations in symmetrical Kikuchi-band contrast are discussed, and the thickness dependence of the angular range with excess contrast is explained. For typical higher-order systematic lines the theory predicts contrast variations similar to the ones found for the band, *i.e.* characteristic thickness-dependent disappearance angles and angle-dependent disappearance thicknesses for the line contrast. The low band contrast observed from very thick specimens is found to be due to the reduced anomalous absorption associated with the higher-order diffuse scattering contributions. Calculated Kikuchi-band contrast due to multiple thermal scattering in Si is given.

Introduction

Bragg scattering effects in diffuse electron scattering, *i.e.* the Kikuchi lines and bands, have been discussed by various authors (Pfister, 1953; Kainuma, 1955; Takagi, 1958; Fujimoto & Kainuma, 1963; Gjønnes, 1966; Hall, 1970; Thomas & Humphreys, 1970; Ishida, 1971; Okamoto, Ichinokawa & Ohtsuki, 1971), and at present the absorption-independent diffraction effects observed from relatively thin crystals are well understood. In particular, qualitative explanations have been given for various effects observed in the narrow lines (Kambe, 1957; Gjønnes & Watanabe, 1966; Uyeda, 1968; Gjønnes & Høier, 1969; Lally,

Humphreys, Metherel & Fischer, 1972; Høier, 1972 *a*, *b*).

In thick crystals and especially for the Kikuchi bands the contrast has been found to depend strongly on anomalous absorption and multiple inelastic scattering effects (*e.g.* Pfister, 1953). Recently a theory was suggested by Thomas & Humphreys (1970) which explained some of the observed effects, in particular the line in the middle of Kikuchi bands frequently observed at high voltages. Their description, however, deviates considerably from observations in the thick-crystal case (Uyeda & Nonoyama, 1967) where the theoretical contrast variation with thickness is the opposite of the observed one. A similar type deviation is found in electron microscopy where the standard many-beam theory gives an overestimate of the anomalous absorption effects.

The failure of existing theories to be valid at any scattering angle and in the whole experimental thickness range seems mainly to be due to the neglect of multiple diffuse scattering. Multiple scattering is particularly important at large scattering angles and in thick crystals (Lenz, 1954), and as multiple scattering and absorption are closely related effects they have to be treated simultaneously. This may especially be important for the available methods for structure-factor determination (Watanabe, Uyeda & Fukuhara, 1968; Gjønnes & Høier, 1971) as the accuracy of these methods are dependent on a precise theoretical description of the diffraction effects utilized.

The purpose of the present studies has been to investigate the influence of multiple diffuse scattering on the contrast of Kikuchi lines and bands in general. The contrast variations with thickness and angle from the incident beam direction have in particular been studied. The theory derived has been applied to calculations of Kikuchi bands in Si due to thermal scattering which gives an important contribution at large scattering angles and in addition can be represented in a convenient analytical form.

Theory

Single diffuse scattering

A theory for diffraction effects in diffuse electron scattering has to include Bragg scattering of the incident beam and multiple diffuse scattering as well as Bragg scattering between the different coupled directions in the background scattering. The following equation for the intensity in the coupled directions $\mathbf{k}_0+\mathbf{s}+\mathbf{h}$ after kinematical single diffuse scattering in a slice dz at depth z in the specimen was derived by Gjønnes (1966):

$$\mathrm{d}I_1(\mathbf{s}+\mathbf{h})=\mathrm{d}z\sum_g\sum_{g'}\sum_f\sum_{f'} S_{hg}(2)S^*_{hg'}(2)f_1(\mathbf{s}+\mathbf{g}-\mathbf{f}) \times f_1^*(\mathbf{s}+\mathbf{g}'-\mathbf{f}')S_{0f}(1)S^*_{0f'}(1)\,. \quad (1)$$

f_1 is a diffuse scattering coefficient and any energy loss accompanying the transition shall here and below be neglected. The Bragg scattering factors are given by the scattering matrix elements, *e.g.*

$$S_{hg}(2)=\sum_j S^j_{hg}(2)=\sum_j C^j_h C^j_g \exp\left[i\gamma^j(t-z)\right]\,. \quad (2)$$

(1) refers to the upper, $(\mathbf{k}_0,z)$, and (2) to the lower part, $(\mathbf{k}_0+\mathbf{s},t-z)$, of the crystal, and C^j_g is a Bloch-wave coefficient associated with the anpassung γ^j. Equation (1) includes both thickness-dependent and thickness-independent terms. The former is important for the interpretation of diffraction patterns from specimens with well defined thicknesses; with variations in the specimen thickness they can be excluded. The Bragg scattering factors in equation (1) will thus only consist of terms of the type $S^j_{hg}(2)\,S^{j*}_{hg'}(2)$ and $S^i_{0f}(1)S^{i*}_{0f'}(1)$. Those with $i=j$ and $i\neq j$ are the intraband and interband terms respectively.

When the incident beam is not very close to a Bragg condition, the dominating factors in equation (1) appear for $f=f'=0$. The number of terms to be included in the summation over band indices is therefore determined from the size of the Bloch-wave intensity excitation coefficients. For the majority of incident beam directions and especially at conventional voltages, one of these, $|B^i_0|^2$, will be much greater than the others [see *e.g.* Fig. 6(*b*)]. A modified equation (1) results, *viz.*

$$\frac{\mathrm{d}I_1(\mathbf{s}+\mathbf{h})}{\mathrm{d}z}=\frac{1}{t}I_1(\mathbf{s}+\mathbf{h})=|B^i_0|^4\sum_g\sum_{g'}\sum_j S^j_{hg}(2) \times S^{j*}_{hg'}(2)F_1(\mathbf{s},\mathbf{g},\mathbf{g}') \quad (3)$$

where

$$F_1(\mathbf{s},\mathbf{g},\mathbf{g}')=f_1(\mathbf{s}+\mathbf{g})f_1^*(\mathbf{s}+\mathbf{g}')\,. \quad (4)$$

B^i_0 refers to the incident beam direction $\mathbf{k}_0$ and $F_1(\mathbf{s},\mathbf{g},\mathbf{g}')$ includes all types of diffuse scattering. These equations correspond to the expressions used by Okamoto *et al.* (1971). If also absorption is included and only two beams are taken into account, the resulting modified equations correspond to the ones given by Hall (1970) and Ishida (1971).

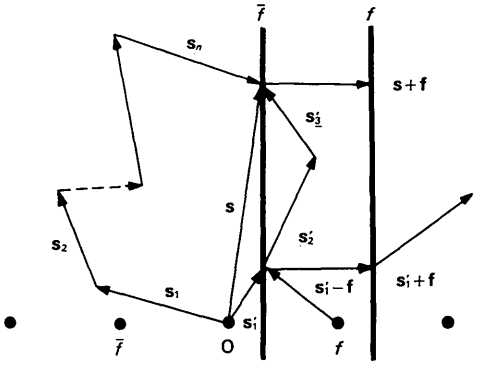

Fig. 1. Different types of multiple diffuse-scattering processes schematically shown.

Diffuse scattering into the particular directions which are associated with the Kikuchi lines and bands, will in such a description only arise from absorption of the discrete beams in the upper part of the crystal. All scattering into these directions at large depths in the crystal due to multiple diffuse scattering, is not included. In thick crystals, however, contributions due to this effect are essential for an interpretation of the observed patterns, as pointed out already by Pfister (1953). We shall now give a theory which takes these contributions into account.

Multiple diffuse scattering

The diffuse background may be more or less modified through Bragg scattering effects depending on the incident beam direction. If the incident beam is close to a low-indices zone axis a complicated Kikuchi line diagram results which covers a large fraction of the angular range usually observed in the electron microscope. Such incident beam directions will not be considered here; attention is focused on the case where only one dense row in reciprocal space is close to the Ewald sphere. The diffuse part of the diffraction pattern therefore essentially consists of a monotonically decreasing background on which a Kikuchi band is superimposed, as shown schematically in Fig. 1.

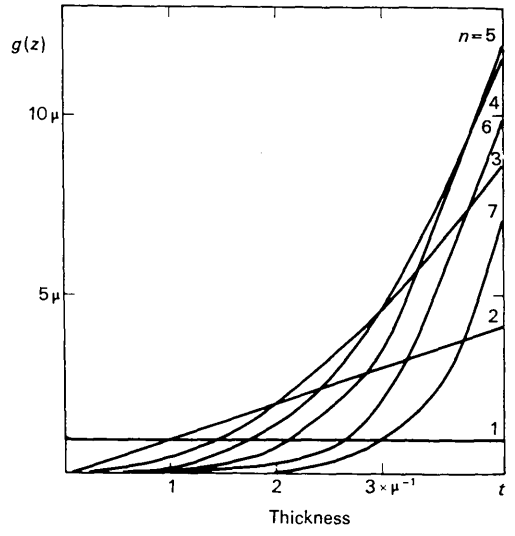

Fig. 2. The variation with thickness of $g(z)=\exp(-\mu z)P_n(z)$, for different values of n.

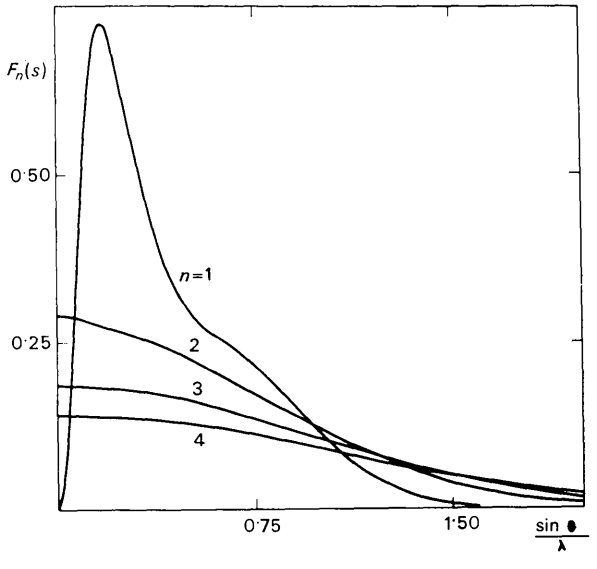

Fig. 3. Multiple thermal scattering distributions. Si.

In addition to single scattering from the direct beam, O, the contributions into the direction $\mathbf{k}_0+\mathbf{s}$ in Fig. 1 are obtained by adding contributions due to multiple intra- and interband scattering from all the other directions $\mathbf{k}_0+\mathbf{s}'$ in the diagram. These can roughly be divided in two types; the directions $\mathbf{k}_0+\mathbf{s}_n'$ which involve Bragg scattering, and the 'random' directions $\mathbf{k}_0+\mathbf{s}_n$ which represent the main part of the observable area. For the latter, which are far from any Bragg condition, only one Bloch-wave component will be non-negligible, see *e.g.* Fig. 6(*b*), and this component can be ascribed to the particular dispersion-surface branch which is close to the zero sphere. The random directions can thus be represented approximately by a plane wave with amplitude close to unity and a wave vector $\mathbf{k}_0^j$ approximately equal to $\mathbf{k}_0$. The corresponding absorption coefficient, μ^j, will be the average coefficient for the specimen.

The following model results: Multiple diffuse background scattering is on the average described by a theory in which Bragg scattering is neglected; only the particular directions $\mathbf{k}_0+\mathbf{s}$ which correspond to the Kikuchi lines and bands, are modified through Bragg scattering and anomalous absorption effects.

The theory of multiple scattering without Bragg scattering, has been discussed by Moliere (1948), Lenz (1954) and Keil, Zeitler & Zinn (1960). It is shown that the intensity can be written:

$$I(\mathbf{s},z)=\sum_n W_n(z)F_n(\mathbf{s}) \tag{5}$$

where W_n, the probability for a particle to be scattered n times after transmission of a specimen with thickness z, is given by the Poisson distribution:

$$W_n(z)=\frac{(\mu z)^n}{n!}\exp(-\mu z)\,. \tag{6}$$

$F_n(\mathbf{s})$ which is the probability for the particle to be observed in the direction $\mathbf{k}_0+\mathbf{s}$ after being scattered n times, can be found from the convolution integrals

$$F_n(\mathbf{s})=\int F_{n-1}(\mathbf{s}-\mathbf{s}')F_1(\mathbf{s}')\mathrm{d}\mathbf{s}' \tag{7}$$

where $n>0$, $F_0(\mathbf{s})=\delta(\mathbf{s})$.

To connect this treatment with a description of Bragg scattering effects, we shall apply a slice approach

similar to the one used above, and treat each nth order contribution independently.

The contribution to the intensity in a direction $\mathbf{k}_0+\mathbf{s}$ after one scattering event in a slice dz at depth z, such that the electron totally has been scattered n times, is written

$$F_n(\mathbf{s})P_n(z)\mathrm{d}z\,.$$

Electrons scattered into the particular directions which are close to Bragg conditions are now separated from the ones in the random directions. The former will be exposed to Bragg scattering and consequently to anomalous absorption on their way out of the crystal, *i.e.* in the thickness $t-z$.

The thickness-dependent quantity $P_n(z)$ is proportional to $W_{n-1}(z)$, the number of electrons scattered $n-1$ times after passing through the thickness z. $P_1(z)$ is hence the quantity which corresponds to the constant prefactor in equation (3). By also taking the absorption factors into account, one obtains a modified equation (3) from which the total single-scattering contribution is obtained through an integration over the crystal thickness, *viz.*

$$I_1(\mathbf{s}+\mathbf{h})=\sum_j\sum_g\sum_{g'} S^j_{hg}(2)S^{j*}_{hg'}(2)F_1(\mathbf{s},\mathbf{g},\mathbf{g}') \times \exp(-\mu^j t)\int_0^t \exp(\mu^j z)P_1(z)\mathrm{d}z\,. \quad (8)$$

This equation, as equation (3) and equivalent expressions in previous theories for Kikuchi lines, is based on the existence of a coherence between the various Bragg scattering factors $S_{hg}(2)f_1(\mathbf{s}+\mathbf{g})$. The higher-order contributions, however, are a result of non-correlated scattering events in the upper part of the crystal. For $n>1$ any coherency is therefore lost, and a relation similar to equation (8) is obtained, including only the terms with $g=g'$. The total intensity can thus be written:

$$I(\mathbf{s}+\mathbf{h})=\sum_j \exp(-\mu^j t)\Big\{\sum_{g\neq g'}\sum S^j_{hg}(2)S^{j*}_{hg'}(2) \times F_1(\mathbf{s},\mathbf{g},\mathbf{g}')\int \exp(-\mu^j z)P_1(z)\mathrm{d}z + \sum_{n>0}\sum_g |S^j_{hg}|^2F_n(\mathbf{s},\mathbf{g})\int \exp(-\mu^j z)P_n(z)\mathrm{d}z\Big\}. \quad (9)$$

The proportionality constant between $P_n(z)$ and $W_{n-1}(z)$ is determined by demanding that this equation transforms to equation (5) for a random direction. We get*

$$P_n(z)=\mu W_{n-1}(z)\,.$$

The integrals in equation (9) which can be found analytically, may profitably be represented by a power expansion in $\Delta\mu^j t$:

$$A^j_n=A_n\Big\{1-\frac{\Delta\mu^j t}{n+1}+\frac{(\Delta\mu^j t)^2}{(n+1)(n+2)} - \frac{(\Delta\mu^j t)^3}{(n+1)(n+2)(n+3)}+\cdots\Big\} \quad (10)$$

where

$$A_n=W_n(z) \quad (11)$$

and

$$\Delta\mu^j=\mu^j-\mu\,.$$

Using equation (2), equation (9) can hence be written:

$$I(\mathbf{s}+\mathbf{h})=\sum_j |C^j_{\mathbf{h}}|^2\{A^j_1\sum_{g\neq g'}\sum F_1(\mathbf{s},\mathbf{g},\mathbf{g}')C^j_g C^j_{g'} + \sum_{n>0}A^j_n\sum_g F_n(\mathbf{s},\mathbf{g})|C^j_g|^2\}\,. \quad (12)$$

where the $C^j_{\mathbf{h}}$'s refer to the direction $\mathbf{k}+\mathbf{s}$. This equation is valid at any scattering angle and crystal thickness. It should be noticed that $F_n(\mathbf{s},\mathbf{g})$ has the form used in kinematical theory which is not the case for $F_1(\mathbf{s},\mathbf{g},\mathbf{g}')$ The latter depends on the presence of Bragg scattering and may for small scattering angles be negative, as pointed out by Gjønnes (1966).

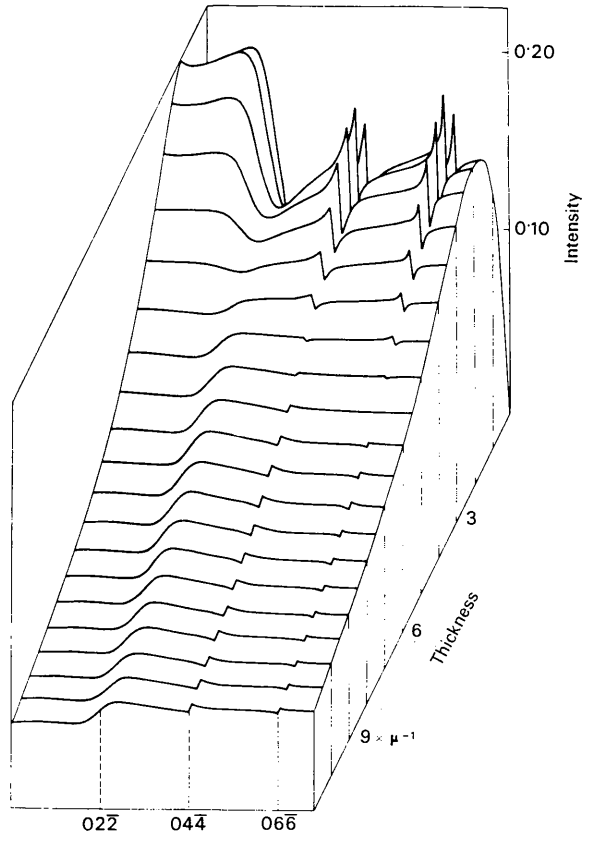

Fig. 4. Calculated half-profiles for the 02$\bar{2}$ band showing thickness dependence for s_{044}.

* In the preliminary calculations (Høier, 1972*a*) a slightly different choice for $P_n(z)$ was made. Qualitatively the previous and present results are the same.

The importance of the higher-order diffuse scattering terms can be seen from the thickness variation of the integrand, $g(z)$, in equation (9). Neglecting anomalous absorption this quantity can be written:

$$g(z)=\exp(-\mu z)P_n(z)\,.$$

The variation in this function with n and z is shown in Fig. 2. For a given direction it is seen that rescattering of the background electrons makes the values of n for the most strongly contributing terms increase with increasing crystal thickness. In thick crystals these terms have typically n values of size μt.

Special cases

Modified intensity expressions which explain the most frequently observed diffraction effects, may be derived from equation (12) through some simplifying assumptions.

For the most common types of excitation $F_1(\mathbf{s})$ has a maximum at or relatively close to $s=0$, and is rapidly decreasing with angle from the incident beam direction. For $n>1$, $F_n(\mathbf{s})$ has a similar variation, but is less strongly peaked about the origin. $F_n(\mathbf{s})$ is thus much greater than $F_n(\mathbf{s}+\mathbf{g})$ if $|\mathbf{s}|\ll|\mathbf{g}|$. In this case one obtains for the *deficient* contrast:

$$I(\mathbf{s})=\sum_n F_n(\mathbf{s})\sum_j |C_0^j|^4 A_n^j \qquad (13a)$$

with the accompanying *excess* contrast

$$I(\mathbf{s}+\mathbf{h})=\sum_n F_n(\mathbf{s})\sum_j |C_0^j C_h^j|^2 A_n^j \qquad (13b)$$

which for negligible anomalous absorption can be written:

$$I(\mathbf{s})=\sum_n F_n(\mathbf{s})A_n\sum_j |C_0^j|^4 \qquad (13c)$$

and

$$I(\mathbf{s}+\mathbf{h})=\sum_n F_n(\mathbf{s})A_n\sum_j |C_0^j C_h^j|^2. \qquad (13d)$$

Comparing these equations with corresponding ones in previous theories, it is found that, *e.g.*, the expressions given by Gjønnes (1966) are similar in form to equations (13*c*, *d*). The sum over all branches which is the important one from a multiple-beam diffraction point of view is equal while the prefactors are different. For an interpretation of observed contrast anomalies, however, this difference is usually eliminated by tilting the crystal until the anomaly of interest has a position on the plate where the background intensity varies slowly with the scattering vector. Alternatively one may use an approximate form by fitting a Gaussian distribution to the experimentally observed background (Høier, 1972*b*).

Using crystal thicknesses which correspond to small anomalous absorption, the inclusion of multiple diffuse scattering will therefore not introduce corrections to existing methods for structure-factor determinations from diffraction effects in Kikuchi patterns. Within the present experimental accuracy estimates indicate that this is also the case in thicker specimens.

The equations (13*a*, *b*) have terms which include factors of the type

$$F_n(\mathbf{s})\frac{(\mu t)^n}{n!}\left(1-\frac{\Delta\mu^j t}{n+1}+\frac{(\Delta\mu^j t)^2}{(n+1)(n+2)}-\cdots\right)e^{-\mu t}\,. \qquad (14)$$

One may here approximate the prefactor of the parentheses by a n-independent function which describe a mean angular variation. If, in addition, the n dependence of the terms in the parentheses is neglected the usual anomalous absorption exponential obtains. The resulting expression is equal to the one obtained taking all diffuse scattering to occur at the entrance surface. This assumption can therefore only be made provided the crystal thickness is small, *i.e.* terms with small n dominate in the intensity expression, and in this case one gets too strong a dependence on the anomalous absorption parameters.

In thick crystals the assumptions leading to equation (13) are no longer valid as $F_n(\mathbf{s}+\mathbf{g})$ cannot be neglected. The full equation (12) has then to be used.

The slow variation in $F_n(\mathbf{s})$ for a large s leads to the approximation $F_n(\mathbf{s})\simeq F_n(\mathbf{s}+\mathbf{g})$ when $|\mathbf{s}|\simeq|\mathbf{s}+\mathbf{g}|$. For this case the different terms in equation (12) can be written:

$$I_1(\mathbf{s})=F_1(\mathbf{s})\sum_j |C_0^j|^2 A_1^j\{1+G_{gg'}^j\} \qquad (15a)$$

and for $n>1$

$$I_n(\mathbf{s})=\sum_{n>1} F_n(\mathbf{s})\sum_j |C_0^j|^2 A_n^j\,, \qquad (15b)$$

where

$$G_{gg'}^j=\sum_{g\neq g'}\sum C_g^j C_{g'}^j\,.$$

The terms given by equation (15*b*) can for small thicknesses be neglected, *i.e.* $I(\mathbf{s})\simeq I_1(\mathbf{s})$ which in the case of negligible anomalous absorption reduces to

$$I(\mathbf{s})\simeq F_1(\mathbf{s})A_1\{1+\sum_j |C_0^j|^2 G_{gg'}^j\}\,. \qquad (15c)$$

This equation corresponds to the expression given by Kainuma (1955) neglecting fine-structure terms. The observed excess bands in thin crystals are due to the asymmetric second factor in the parentheses. This factor is usually positive inside the band, *i.e.* between the first-order lines, and negative immediately outside.

While equation (15*a*) gives an excess band, equation (15*b*) gives always a deficient band. The resulting contrast therefore depends on several factors; two important ones are the crystal thickness which is included in A_n^j, and the scattering angle through $F_n(\mathbf{s})$. From equation (7) it follows that the width of $F_n(\mathbf{s})$ increases with n. Thicknesses can therefore be found for which equation (15*b*) dominates at large scattering angles while $I_1(\mathbf{s})$ dominates at smaller angles giving deficient and excess contrast respectively. At an intermediate s a disappearance angle, β_1, for the band contrast is found. β_1 is thickness-dependent and decreases

with t. β_1 should not be mistaken for another disappearance angle α_1, which appears in the low-angle region where equation (15) is not valid. This angle, below which a deficient band is observed, is essentially due to the sign of the quantity $F_1(\mathbf{s},\mathbf{g},\mathbf{g}')$ in equation (12) for small scattering angles (Ishida, 1971; Okamoto *et al.*, 1971). The angle α_1 increases with the crystal thickness as shown recently by Komuro, Kojima & Ichinokawa (1972).

The angular extent, $\beta_1-\alpha_1$, of the area with excess contrast therefore decreases with crystal thickness owing to the corresponding reduction in the first-order contribution. At larger t only a deficient band is observed. The previously unexplained contrast variations of Kikuchi bands along their length are therefore at present understood.

It follows from the discussion above that scattering angles can always be found for which $I_1(\mathbf{s})$ dominates at small t and the $n>1$ contributions at large t. In accord with the observations of Pfister (1953), the contrast for constant s is therefore continuously decreasing with increase in crystal thickness, and an angle-dependent disappearance thickness for the band contrast is obtained.

The approximations which were discussed in connexion with equation (14), may also be applied in equation (15*b*). Terms of the type $|C_0^j|^2\exp(-\mu^j t)$ result, and we get an intensity expression equal to the one suggested by Thomas & Humphreys (1970) if the angle-dependent prefactor is either taken to be constant or approximated by an experimentally determined distribution. As shown above, such a description can only be applied for small n, *i.e.* for thicknesses where $I_1(\mathbf{s})$ is non-negligible. Applied to cases were $I_1(\mathbf{s})$ is small, however, this theory gives a qualitative explanation of the observed channelling effects; but a reasonable fit between theory and experiment can only be obtained in the intermediate crystal-thickness range.

As multiple diffuse scattering is only taken into account phenomenologically in the theory of Thomas & Humphreys (1970), in such a way that all electrons are exposed to anomalous absorption in the total crystal thickness, the deviation from the observed contrast will increase with thickness for large thicknesses; in the limit non-negligible intensity is only predicted in the well channelled directions. Having the same thickness variation a similar overestimate of the anomalous absorption effects is obtained for bend contours. In both cases this is due to the neglection of the multiple-scattering contributions at great depth in the crystal. These are included in equation (15) which gives a reduced contrast at large thicknesses in accord with observations (Uyeda & Nonoyama, 1967).

Calculations

The scattering functions $F_n(\mathbf{s},\mathbf{g},\mathbf{g}')$ generally include all types of background scattering such as phonon, plasmon, single-electron scattering, disorder scattering *etc.*, and convolutions between different processes may also be included. We shall here limit the discussion to a simple example, *i.e.* multiple phonon scattering. This type of background scattering represents an important contribution at large scattering angles and can further be expressed in a convenient analytical form using the method given by Hall & Hirsch (1965), with the analytical representation of atomic scattering amplitudes given by Smith & Burge (1962). The integration in

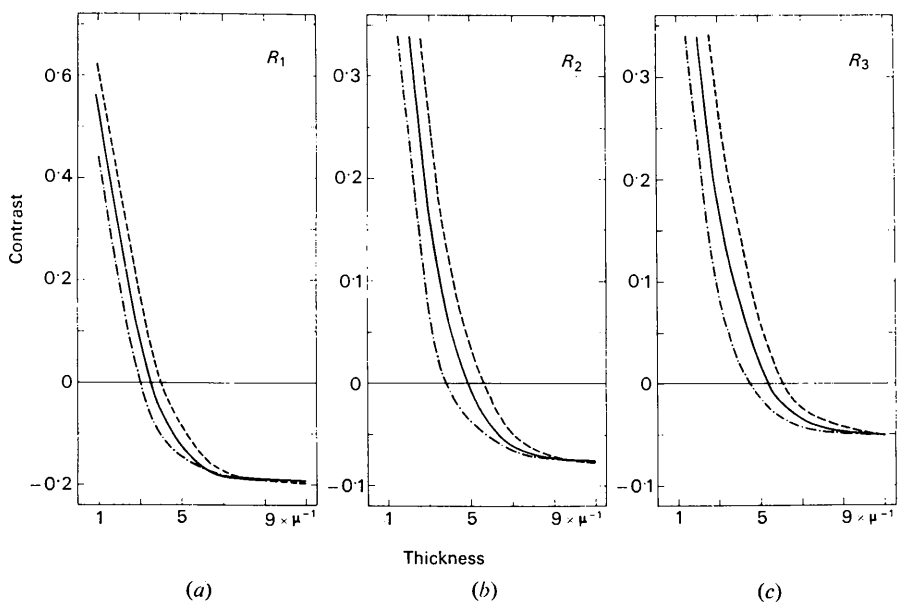

Fig. 5. Calculated contrast as a function of thickness for s_{022}: dashed curves, s_{044}: full curves and s_{088}: dash-dot curves (*a*) $02\bar{2}$ band contrast (*b*) $04\bar{4}$ contrast (*c*) $06\bar{6}$ contrast.

equation (7) is approximated to include all $\mathbf{s}'$ in a plane normal to $\mathbf{k}_0$ giving $F_n(\mathbf{s})$ as a sum over exponentials. The resulting diffuse scattering distributions for Si at room temperature and 100 kV, are shown in Fig. 3 for $n=1$ to 4. $F_1(\mathbf{s})$ which for thermal scattering is negligible at small angles, has a maximum value near $(\sin\theta)/\lambda = 0{\cdot}2$ Å^{-1} and is rapidly decreasing with angle for $(\sin\theta)/\lambda \gtrsim 1$ Å^{-1}. The effect of subsequent thermal scattering is to smear out this distribution in favour of scattering to very small and in particular to higher angles. This is the origin of the observed net flow of background electrons outwards in diffraction patterns when the crystal thickness is increased, *i.e.* increasing the probability of higher-order scattering.

The $02\bar{2}$ and $11\bar{1}$ Kikuchi-band contrasts from Si have been calculated from equation (15). In all examples 12 interacting beams have been used and all terms with $n=1$ to 16 are included. The Fourier coefficients for the real and imaginary part of the potential have been taken from Radi (1970).

The $02\bar{2}$ band

Half profiles for the $02\bar{2}$ band including the higher-order lines have been calculated for different thicknesses and angles from the incident beam direction. The angle is below expressed by the quantity s_{hkl} which is equal to the length of the reciprocal-lattice vector with the corresponding indices.

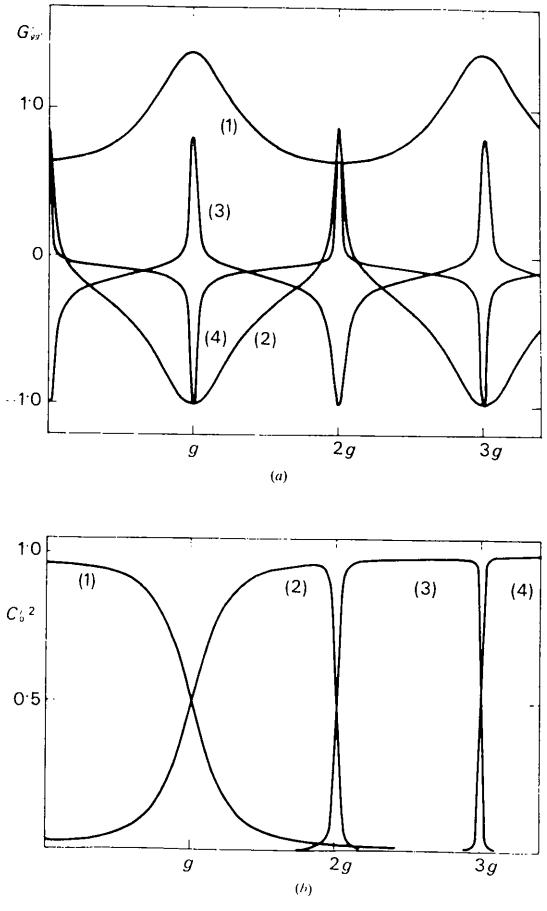

Fig. 6. Calculated variations in (*a*) G^j_{gg} (see text) and (*b*) excitation coefficients with beam direction. $g=02\bar{2}$.

The dependence of band contrast on thickness for s_{044} is shown in Fig. 4. The band appears with excess contrast at small thicknesses and deficient contrast at large thicknesses, the thickness of zero contrast being close to $\mu t = 3{\cdot}5$. As a measure of contrast we shall use the quantity R_n where n is the order of the line, *i.e.* $n=1$ for the band, $n=2$ for the second-order line *etc.*,

$$R_n = 2\,\frac{I_n(\text{i.s.}) - I_n(\text{o.s.})}{I_n(\text{i.s.}) + I_n(\text{o.s.})}\,.$$

For $n>1$ the intensities introduced in this equation are the extreme intensity values immediately inside (i.s.) and outside (o.s.) the ordinary line position; for the band contrast the intensities used are the ones halfway between the middle of the band and the band edge, and halfway between the first and second-order lines.

R_1 as a function of thickness for various scattering angles is shown in Fig. 5(*a*). For a given s the contrast is continuously decreasing with thickness up to $\mu t \simeq 9$ with an s-dependent disappearance thickness between $\mu t = 3$ and 4. Above a thickness interval with close to constant R_1, the contrast, *i.e.* $|R_1|$, slowly decreases.

The thin-crystal contrast is determined by the single-scattering contribution only, *i.e.* equation (15*c*), and the two important factors in this equation are shown in Fig. 6. The variations in the Bloch-wave intensity excitation coefficients shown in Fig. 6(*b*), are typical for conventional voltages and metals with atoms of relatively low atomic numbers, *i.e.* apart from the directions close to Bragg conditions, one excitation coefficient is much greater than the others. Within the band, the dominating branch-1 contribution will be positive as the sum $G^j_{gg'}$ [Fig. 6(*a*)] here is positive. Moving towards the band edge $G^j_{gg'}$ increases more rapidly than $|C^j_0|^2$ decreases and a maximum immediately inside the first-order Bragg position obtains. The minimum value outside the band is due to the negative branch-2 contribution combined with the decrease in the branch-1 value.

As shown above the thick-crystal contrast is determined by the $n \gg 1$ terms. The reduced anomalous absorption obtained is therefore due to scattering at large depths in the crystal from random directions into the band directions.

The calculated $02\bar{2}$ band contrast as a function of s for $\mu t = 3{\cdot}5$ is shown in Fig. 7, where a deficient band appears at small and large scattering angles. For this thickness a disappearance angle for thermal scattering is hence found at $\beta_1 \simeq s_{066}$. Another angle corresponding to the one denoted α_1 above, seems to be predicted at low angles (see dotted curves in Fig. 7). Here, however, the assumption leading to equation (15) breaks down and equation (12) has to be used.

The $02\bar{2}$ *higher-order lines*

As for the band, we can for the contrast of higher-order lines distinguish between thin-crystal and thick-crystal profiles; the first type being due to the single-scattering contribution while the latter can be ascribed to the $n>1$ terms. At any thickness, the higher-order lines are asymmetric as shown in Fig. 4. In a thin crystal the maximum in the asymmetric line is found immediately inside the ordinary line position, and the minimum immediately outside, while the contrast is reversed in the thick-crystal case. Both profile types can be understood from Fig. 6. The first type is essentially an absorption independent effect, [equation (15*c*)], and the maximum in, *e.g.*, the second-order line is due to the maximum value in the product $|C_0^2|^2 G_{gg}^2$, inside the line position, whereas the intensity on the other side of the line position results from the minimum in the same product for branch 3. The reversed contrast of the second-order line in a thick crystal is due to the strong absorption of branch 2 inside and low absorption of branch 3 outside the line position.

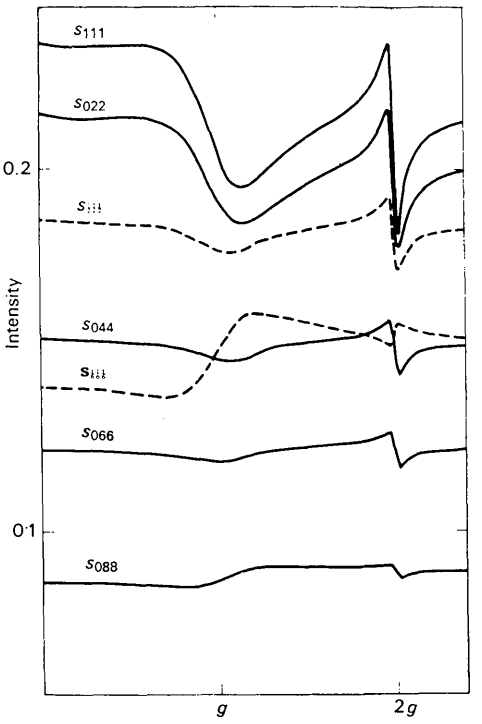

Fig. 7. Calculated band-intensity variations with scattering angle for $\mu t=3{\cdot}5$. $g=02\bar{2}$

For a given scattering angle, the thickness of zero contrast will depend on the line considered as different branches and consequently different absorption parameters are involved for *e.g.* the second and third-order lines. This effect can be seen from Fig. 5 (*b*) and (*c*) where the disappearance thickness for the second-order line is varying from $\mu t=5{\cdot}6$ to $3{\cdot}8$ when the scattering angle changes from s_{022} to s_{088}. The corresponding values for the third-order line are $\mu t=6$ and $4{\cdot}5$.

The contrast variations with angle for constant thicknesses are shown in Fig. 8 (*b*) and (*c*). These curves have a similar type variation as R_1. Fig. 8 (*a*) shows that R_1 is less than zero for $\mu t=5$ independent of scattering angle. R_2, however, is equal to zero for $\alpha_2'=0{\cdot}35\ s_{022}$ and $\beta_2=1{\cdot}42\ s_{02\bar{2}}$, and $R_3=0$ for $\alpha_3'=0{\cdot}27\ s_{022}$ and $\beta_3=3{\cdot}27\ s_{022}$. From the variation in β_n it is thus found that the angular extent of thin-crystal contrast is increasing with increasing line order. The angles α_n' appear as above at small angles where the intensity

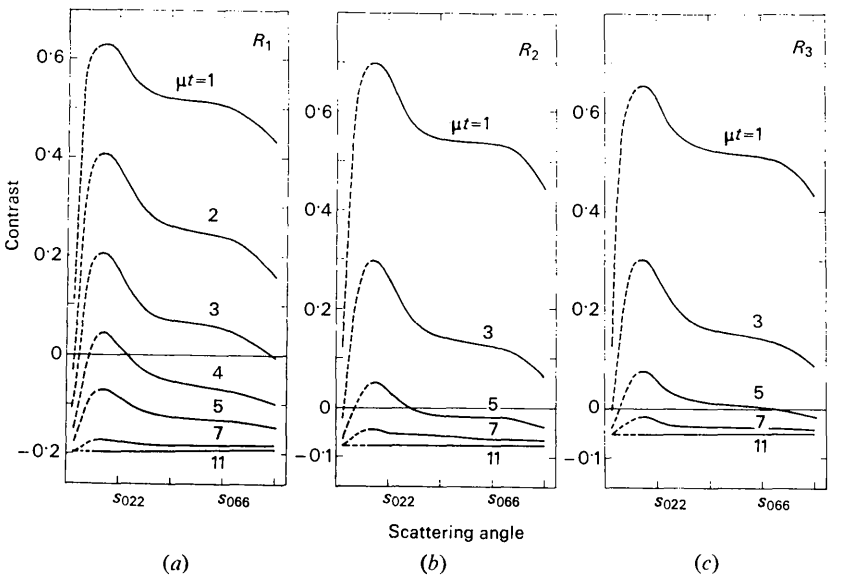

Fig. 8. Calculated contrast dependence on scattering angle for various thicknesses. (*a*) $02\bar{2}$ band contrast. (*b*) $04\bar{4}$ contrast (*c*) $06\bar{6}$ contrast.

expression used represents an oversimplification, and the full equation (12) has to be applied.

Both the size and the line-order dependence of the disappearance angles and thicknesses essentially reflect differences in the anomalous absorption parameters.

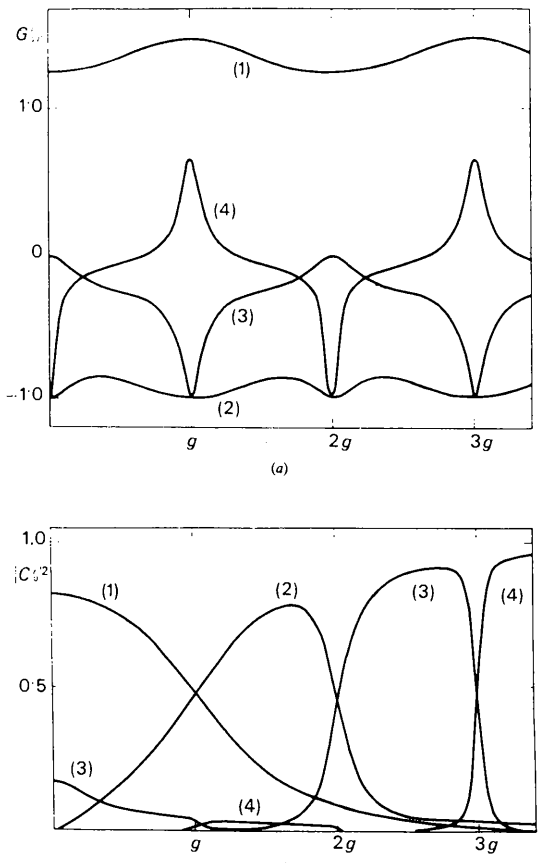

Fig. 9. Calculated variations in (*a*) $G^J_{gg'}$ and (*b*) excitation coefficients with beam direction. $g = 11\bar{1}$.

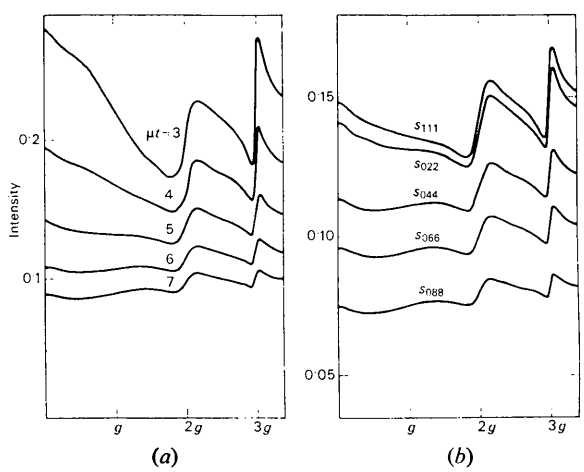

Fig. 10. Calculated band-intensity variations for $g = 11\bar{1}$. (*a*) $s_{02\bar{2}}$. (*b*) $\mu t = 5$.

The influence of changes in μ^J on these angles has so far not been investigated; it seems feasible, however, to subtract information about absorption parameters from the contrast variations described.

The $11\bar{1}$ *band*

The 111-type bands in Si are known to have double the normal width (Fowler & Marton, 1965), and it has been shown by Thomas & Humphreys (1970) that the same effect is observed as well for most metals at high voltages. This contrast in Si at conventional voltages which is mainly due to the difference in sign of the first and third-order structure factors, can be understood from the calculated excitation coefficients and $G^J_{gg'}$ shown in Fig. 9. The latter factors are approximately constant for branches 1 and 2, the signs being different, however, while the branch-1 excitation coefficient has a close to linear dependence on distance from the band centre up to the second-order line position. For the thin-crystal case one therefore obtains an excess band with approximately linearly decreasing intensity up to the second-order line positions, as shown in Fig. 10(*a*).

With increasing crystal thickness the anomalous absorption leads to an enhanced importance of the branch-3 contributions. From Figs. 9 and 10, it is seen that these contribute in the middle of the band, and outside the second-order line position, *i.e.* the branch-3 channelling directions.

Calculated profiles for different scattering angles are shown in Fig. 10(*b*) where $\mu t = 5$. The reduction in anomalous absorption attributable to the higher-order terms is here reflected in the contrast variations of the central line. The contrast which has its maximum at intermediate scattering angles, is seen to decrease slowly with s. This is a typical variation which is expected to be found in the patterns independent of acceleration voltage.

It should be noted that the third-order line appears with $R_3 < 0$, independent of crystal thickness. Negative contrast for small thicknesses originates here from the signs of $G^J_{gg'}$, $j = 3$ and 4, which is opposite to the corresponding ones in the $06\bar{6}$ case.

Conclusions

For an interpretation of diffraction patterns intensity contributions attributable to multiple diffuse scattering are essential if either the crystal thickness or the scattering angle is large. Such contributions are included in the present theory, which represents a unified description of multiple diffuse scattering and Bragg scattering effects. Compared with theories given previously for the contrast in Kikuchi line patterns the present intensity expressions are found to include the ones derived by *e.g.* Kainuma (1955), Gjønnes (1966) and Thomas & Humphreys (1970).

Applied to thin, non-absorbing crystals essential differences between the present and previous theories

have not been found. No corrections are therefore introduced to available methods for structure-factor determination from diffraction effects in weak, narrow lines.

In thick crystals the present description deviates considerably from previous ones. This deviation is found to arise from the inclusion of the higher-order diffuse-scattering terms being due to scattering into the particular directions associated with the Kikuchi lines and bands at large depths in the crystal. Reduced anomalous absorption results in accord with observations.

The contrast dependence on angle from the incident beam direction is for all thicknesses found to be dependent on the higher-order diffuse-scattering contributions which appear with increasing order with increase in angle. The previously unexplained variations in the contrast of symmetrical Kikuchi bands along their length are thus at present understood. In addition to the change from deficient to excess contrast found at small angles (Okamoto *et al.*, 1970) a disappearance angle for the band contrast is predicted at a larger angle. Here the band contrast changes back to deficient when the $n > 1$ terms start to dominate over the single-scattering term. The extent of the area with excess contrast is hence found to decrease with increasing crystal thickness.

Typical profiles for the higher-order lines are found to have a similar variation to the band with thickness and scattering angle, *i.e.* thickness-dependent disappearance angles and angle-dependent disappearance thicknesses. A similar type inversion of contrast is reported by Thomas (1972) for the second-order line when going through the disappearance voltage. To separate this effect from the present ones care has therefore to be taken to ensure that equal-thickness patterns are compared.

In electron microscopy from thick crystals electrons which have been exposed to multiple scattering inevitably contribute to the image. An extension of the present theory to bend-contour calculations is therefore suggested. For defect studies it was found by Uyeda & Nonoyama (1967) that the experimental maximum thickness corresponds to a thickness where reduced anomalous absorption is observed in the Kikuchi band. This correspondence shows that calculations of defect contrast in thick crystals have to be based on a diffraction theory which takes multiple diffuse scattering into account; applications of the present theory for such calculations have so far not been investigated.

The author is grateful to Dr J. Gjønnes for stimulating discussions.

References

FOWLER, H. A. & MARTON, L. (1965). *J. Appl. Phys.* **36**, 1986–1995.

FUJIMOTO, F. & KAINUMA, Y. (1963). *J. Phys. Soc. Japan*, **18**, 1792–1804.

GJØNNES, J. (1966). *Acta Cryst.* **20**, 240–249.

GJØNNES, J. & HØIER, R. (1969). *Acta Cryst.* A**25**, 595–602.

GJØNNES, J. & HØIER, R. (1971). *Acta Cryst.* A**27**, 313–316.

GJØNNES, J. & WATANABE, D. (1966). *Acta Cryst.* **21**, 297–302.

HALL, C. R. (1970). *Phil. Mag.* **22**, 63–72.

HALL, C. R. & HIRSCH, P. B. (1965). *Proc. Roy. Soc.* A**286**, 158–177.

HØIER, R. (1972*a*). *Proc. Fifth. Europ. Conf. Electron Microsc. Manchester*, pp. 444–445.

HØIER, R. (1972*b*). *Phys. Stat. Sol.* (*a*), **11**, 597–610.

ISHIDA, K. (1971). *J. Phys. Soc. Japan*, **30**, 1439–1448.

KAINUMA, Y. (1955). *Acta Cryst.* **8**, 247–257.

KAMBE, K. (1957). *J. Phys. Soc. Japan*, **12**, 13–31.

KEIL, E., ZEITLER, E. & ZINN, W. (1960). *Z. Naturforsch.* **15a**, 1031–1038.

KOMURO, M., KOJIMA, S. & ICHINOKAWA, T. (1972). *J. Phys. Soc. Japan*, **33**, 1415–1419.

LALLY, J. S., HUMPHREYS, C. J., METHERELL, A. J. F. & FISCHER, R. M. (1972). *Phil. Mag.* **25**, 321–343.

LENZ, F. (1954). *Z. Naturforsch.* **9a**, 185–204.

MOLIERE, G. (1948). *Z. Naturforsch.* **3a**, 78–97.

OKAMOTO, K., ICHINOKAWA, T. & OHTSUKI, Y. (1971). *J. Phys. Soc. Japan*, **30**, 1690–1701.

PFISTER, H. (1953). *Ann. Phys.* **11**, 239–269.

RADI, G. (1970). *Acta Cryst.* A**26**, 41–56.

SMITH, G. M. & BURGE, R. E. (1962). *Acta Cryst.* **15**, 182–186.

TAKAGI, S. (1958). *J. Phys. Soc. Japan*, **13**, 278–296.

THOMAS, L. E. & HUMPHREYS, C. J. (1970). *Phys. Stat. Sol.* (*a*), **3**, 599–615.

THOMAS, L. E. (1972). *Phil. Mag.* **26**, 1447–1465.

UYEDA, R. (1968). *Acta Cryst.* A**24**, 175–181.

UYEDA, R. & NONOYAMA, M. (1967). *Jap. J. Appl. Phys.* **6**, 557–566.

WATANABE, D., UYEDA, R. & FUKUHARA, A. (1968). *Acta Cryst.* A**24**, 580–581.